DOI: 10.1002/((please add manuscript number))

Article type: Communication

New Strategy to Overcome the Instability That Could Speed up the Commercialization of Perovskite Solar Cells

*Omid Amiri, Amir Ehsan Rezaee, Hakimeh Teymourinia, Masoud Salavati-Niasari, L Jay Guo *, Ardashir Baktash*

Dr. O. Amiri

Chemistry Department, College of Science, University of Raparin, Rania, Kurdistan Region, Iraq

Dr. A. Rezaee, Dr. H. Teymourinia, Prof. M. Salavati

Institute of Nano Science and Nano Technology, University of Kashan, Kashan, P. O. Box. 87317-51167, I. R. Iran
E-mail: salavati@kashanu.ac.ir

Prof. L. J. Guo
Department of Electrical Engineering and Computer Science

University of Michigan

Ann Arbor, MI 48109, USA

E-mail: guo@umich.edu

Ardashir Baktash

Centre for Theoretical and Computational Molecular Science, Australian Institute for Bioengineering and Nanotechnology, The University of Queensland, Brisbane, QLD, 4072, Australia.

Keywords: mechanism; stability; degradation; Perovskite Solar Cell

Current efficiency of perovskite solar cells has reached 23.7%, which is comparable with silicon solar cells. However commercial development is seriously hindered by the instability of the perovskite, especially under moisture conditions. Therefore it is crucial to gain clear understanding of the mechanism of degradation of Organic-inorganic perovskite in order to achieve stable perovskite devices. In this paper, the formation and the degradation of perovskite film on different charge transport layers such as a compact TiO_2 layer, compact ZnO layer, and ZnO foil, Si Nanowires (NWs) and porous Si were studied. In addition, Density Functional Theory (DFT) studies were carried out to better understand the interaction between the perovskite film and substrates. We combine experimental and theoretical results to draw more reliable conclusion regarding the degradation mechanism. Most notably, our investigations show that the interaction between the iodine (I) atom in the perovskite layer and substrate determine the stability of perovskite cells. As a result, Si has minimum interaction with I atoms and showed maximum stability, while perovskite film degrades on TiO_2 film almost immediately.

Since 2009, organic-inorganic perovskite solar cells (PSCs) have increasingly attracted attention because of the advantages it offered in long charge diffusion lengths obtained, simple fabrication procedures, low price of raw materials and sustainability, and have enjoyed rapid rise in efficiency. [1-8] Since 2009, the main research was focused on improving the efficiency of perovskite solar [9-12] which lad to reported efficiency up to 23.7%. [13] Current efficiency is comparable with commercial Si solar cells. The main barrier to entry for perovskite solar cells into the market is their instability. This is the reason why recent research have been focusing on improving the stability of perovskite solar cells. [14-17] However, the problem of low stability remains unsolved. Organic-inorganic perovskite degraded under light illumination, in the presence of moisture and thermal stress. [18-20] There have been a great amount of efforts to improve the stability of perovskite solar cells. [21-24] For example

Gratzel et al. replaced MA with Cs and Fa that led to improved stability. [25] According to their report, $FA_{0.9}Cs_{0.1}PbI_3$ film was stable for 19 h under ambient condition. In another report, Saliba and Co-workers show that $Cs_x(MA_{0.17}FA_{0.83})_{(1-x)}Pb(I_{0.83}Br_{0.17})_3$ film is stable for 250 h under operational conditions. [26] It is important to have a clear understanding of the mechanism of formation and degradation of Organic-inorganic perovskite in order to search for solutions to stable perovskite photovoltaic devices. Despite the efforts by many researchers in the last three years. [27-37], the exact mechanism for degradation of Organic-inorganic perovskite remained unclear. In 2014, Wang and co-workers reported that the first step in perovskite decomposition is the reversible deprotonation of the MA cation by water, where H_2O gets proton from MA cation and converts to H_3O^+ whereas MA converts to CH_3NH_3I. [38] In late 2014, Nishino et al. showed that under irradiation perovskite $MAPbI_3$ was converted to PbI_2, by releasing CH_3NH_2 and HI molecules. [39] On the other hand, in 2015 Kelly et al. disagreed with Wang's mechanism and argued that the initial step of the perovskite decomposition process is not an acid-base reaction involving the MA ($CH_3NH_3^+$ =MA) cation but is rather a hydration process of the perovskite film. [40] Later Philippe et al. rejected the hypothesis proposed by Kelly et al., as they found that the perovskite material decomposed into PbI_2 not only in a humid air but also in inert gases such as argon. [41] After that, Sit et al. suggested a new mechanism for the degradation of Organic-inorganic perovskite, [42] by performing an Ab Initio Study and suggested that the degradation of perovskite started with the interaction between OH radical or OH anion with MA cation. [43] They declared that the OH radical or OH anion take H radical or H proton to form H_2O and CH_3NH_3PbI. In 2016, Nie et, al. proposed a new mechanism for the degradation of perovskite under light, [43] in that the light-activated meta-stable deep-level trap states are responsible for the degradation of the perovskite layer under light irradiation. In the same year,

Snaith and et, al. suggested that superoxide react with MA cation and degraded $CH_3H_3PbI_3$ [4441]. Very recently, Walsh et, al. investigated the origin of perovskite decomposition through point defect processes in water-intercalated $MAPbI_3$, denoted as $MAPbI_3\_H_2O$ hereafter, and monohydrated phase, $MAPbI_3 \cdot H_2O$. The water-intercalated $MAPbI_3\_H_2O$ is suggested as an intermediate phase during the transition to the hydrated phases due to the relatively low activation energies for water insertion into the perovskite surface. [45]

All of these proposed mechanisms focused on the interaction between extrinsic factors such as moisture, superoxide, OH radical with the perovskite film. Also, all the previous degradation studies focused on one ETL only where the researchers drew their conclusions. Also, the formation mechanism of the perovskite layer rarely is discussed, while we believe that it is necessary to understand the how the perovskite crystals are formed on the substrate in order to gain better understanding of the degradation mechanism. Herein we investigate the degradation of perovskite absorber layer on different ETL layers such as a compact TiO_2 layer, compact ZnO layer, and ZnO foil, Si NWs and porous Si and suggest a formation mechanism of the perovskite layer. In addition, we performed DFT calculations to assist our experimental studies to reach a more reliable conclusion regarding the degradation mechanism. Our investigations have revealed that the interaction between the iodine (I) atom in the perovskite layer and substrate determine the stability of perovskite cells. For example, Si has minimum interaction with I atoms and showed maximum stability, whereas perovskite film degrades on TiO_2 film almost immediately. We also show that degradation of perovskite films are reversible process even in the presence of water, while previous reports mentioned that perovskite films are only reversible when humidity is below 80%. [34, 40]

In the present work, we want to introduce a new mechanism for the degradation and formation of perovskite solar cell which could explain all behaviors of perovskite solar cells. For this, we first

studied the degradation of perovskite absorber layer ($CH_3NH_3PbI_3$) on compact TiO_2 layer, compact ZnO layer and ZnO foil, Si NWS and porous Si. Degradation of $CH_3NH_3PbI_3$ on each layer was monitored for three days by means of XRD. XRD of the substrates is shown in **Figure S1** in the supporting information. Related results are presented in **Figure 1, 2**. **Figure 1 a** show the degradation of $CH_3NH_3PbI_3$ on TiO_2 substrate. Here we consider intensity ratio of the peak at~12˚and~14˚(R P/M) over time to evaluate the degradation rate. It should be noticed that peaks located at 12.7˚and 14.1˚belong to the PbI_2 and $CH_3NH_3PbI_3$ phase, respectively. In the case of TiO_2, this ratio after 1 day is about ½ and a significant amount of $CH_3NH_3PbI_3$ converted to PbI_2. In the third day after synthesis of $CH_3NH_3PbI_3$ on TiO_2, this ratio increased to 1/1. XRD pattern of $CH_3NH_3PbI_3$ on compact ZnO was illustrated in **Figure 1 b**. After 2 days, this ratio increased to ¼. By monitoring the degradation of $CH_3NH_3PbI_3$ for 3 days, we found that this ratio increased to 2/3. While for $CH_3NH_3PbI_3$ deposited on the ZnO foil, R P/M is 1/3 and 1/2 after 1 day and 2 days, respectively (**Figure 1 c**).

Figure 2 a summarized XRD patterns of $CH_3NH_3PbI_3$ on single crystal Si NWs for 30 days. The reason for the 30 days monitoring was because we did not observe any peak at 12/7˚for the first 3 days. Interestingly even after 30 days P/M is~0. In other words, $CH_3NH_3PbI_3$ is highly stable on Si NWs. The same results were obtained for $CH_3NH_3PbI_3$ on the porous polycrystalline silicon (**Figure 2 b**), with no conversion to PbI_2. This illustrates that the degradation of perovskite mainly depends on the material of substrate rather than its morphology. SEM images of porous Si NWS and porous Si are illustrated in **Figure S2**.

The Morphologies of the perovskite films were studied by using scanning electron microscopy (SEM). SEM images of $CH_3NH_3PbI_3$ deposited on different substrates are shown in **Figure 3 a-c**, where it can be seen that the morphology of perovskite films on different substrates are the same. Atomic force microscopy (AFM) was also used to study the topography of perovskite deposited on

different substrates. As seen from the AFM results, all samples almost have the same topography (**Figure 3 e-f**). Because the morphology and topography of $CH_3NH_3PbI_3$ on different substrates are almost the same. We believe that the interaction between I atoms in the perovskite layer and substrate determine the stability of perovskite layer.

DFT analysis was carried out to better understand the interaction between the perovskite and substrate. Detail of the computational method could be found in the computational method section. We study the interaction between the perovskite layer and Si, ZnO, and TiO_2, reflected by E_{ab}, which was calculated according to eq.1.

eq 1) $E_{ab} = E_{S\text{-}Pv} - (E_S + E_{Pv})$

Here, $E_{S\text{-}Pv}$, E_S and E_{Pv} show the energy of substrate/perovskite, energy of substrate and energy of perovskite, respectively. E_{ab} for perovskite deposited on TiO_2 was 1.85 eV. Interaction between perovskite and ZnO is close to those of TiO_2 (E_{ab} =1.83 eV), while E_{ab} for perovskite deposited on Si is only 0.78 eV. As seen from **Figure 4**, the perovskite layer connects to the substrate via the I atom in TiO_2 and ZnO. These computational results corroborate our experimental results: we believe that the degradation started by the weakening of interaction between cation ($CH_3NH_3^+$) and anion (PbI_3^-) in the perovskite. This happens when perovskite has significant interaction with the substrate. For example, TiO_2 substrate has the highest interaction (this interaction is between TiO_2 and I atom in the perovskite anion) which leads to decreased interaction between $CH_3NH_3^+$ and PbI_3^-. **Figure 5** shows the degradation mechanism for TiO_2 which starts by the interaction between the perovskite layer and substrate which leads to weakening of the bond between the PbI_3 anion and CH3NH3 cation. Extrinsic factors such as oxygen and water can react with $CH_3NH_3^+$ when the bond between CH_3NH3^+ and PbI_3^- is weakened. Si substrate and I atom in perovskite has lower interaction energy than TiO_2 and ZnO.

Perovskite on silicon shows the highest stability because CH_3NH_3 cation has interaction with substrate instead of I atom. In this situation, extrinsic factors could not attack the CH_3NH_3 cation.

This mechanism introduced above is applicable to previous reports. For instance, Nishino et al reported that device with Sb_2S_3 on TiO_2 was stable for 12 h under light exposure, while reference cell converted to PbI_2 in the same time [40]. This stability comes from lower interaction between Sb_2S_3 and perovskite. In fact, Sb_2S_3 postpone the first step in the degradation of perovskite. The paper published by Cao shows that this mechanism exactly works for other situation [46]. In this work, protonated ethanolamine was used as a linker between ETL and perovskite layer, which minimized the interaction between ETL and perovskite and improved stability of perovskite solar cells.

Perovskite layer was formed on ZnO very quickly. The formation rate on TiO_2 was slower than ZnO. The lowest formation rate belonged to the Si (perovskite layer needs 24 h to form on Si). We believe that the first step in the formation of the perovskite layer is interaction of PbI_2 with substrate. Based on HSAB theory Zn^{+2} (d10) is a soft cation and I is a soft anion (soft refers to easily polarizable), therefore, they have better interaction and we can consider this whole system (ZnO/PbI_2) as soft complex [47, 48]. This soft complex has better interaction with I in the CH_3NH_3I and show the fastest reaction rate. In the case of TiO_2, Ti_4^+ (d0) is hard cation, therefore, TiO_2/PbI_2 is hard complex which leads to decreased reaction rate. In the other hand, Si does not have significant interaction with PbI_2 and shows the lowest reaction rate. **Figure 6** schematically shows the mechanism for the formation of perovskite layer on different types of substrates.

To further prove the stability of perovskite depends primarily on the type of substrate, reversibility of perovskite structure was tested in direct contact with water. For this, 2 µl of water dropped on perovskite film deposited on different substrates. This was done on hot plate (see video in the

supporting information). While the previous reports declared that perovskite films were reversible in humidity above 80%, we show that this actually depends on the substrate. **Figure 7** shows the XRD pattern and Diffuse Reflectance Spectroscopy (DRS) of perovskite on the different substrate before and after contacting with water. Intensity of peak at ~12 for perovskite on TiO_2 and ZnO decreased after contacting with water, while, it remained almost constant for perovskite on Si. Absorption of perovskite on TiO_2 and ZnO decreased after contacting with water, while almost constant for perovskite on Si.

In conclusion, to understand the mechanism of degradation of Organic-inorganic perovskite for photovoltaic application, all of pervious proposed mechanisms focused on interaction between extrinsic factors such as moisture, superoxide, OH radical etc with perovskite film. This work shed light on the mechanism of degradation in perovskite solar cells by investigating the degradation of perovskite film on different layers such as compact TiO_2 layer, compact ZnO layer and ZnO foil, Si NWS and porous Si; and coupled with DFT calculation to better understand the interaction between perovskite film and substrate materials. Base of theoretical and experimental results, we found that interaction between I atom in perovskite layer and substrate determine the stability of perovskite cells. This new understanding will provide important guidelines on how to develop perovskite solar cells with long terms stability suitable for commercial applications.

Experimental Section

Deposited $MAPI_3$ on different substrates: All substrates were pre-cleaned before using. Here $MAPI_3$ was deposited on FTO/TiO_2, Si NWS, FTO/ZnO, Zn foil by drop casting method (schematic

S1 shows the method for deposition of $MAPI_3$ on TiO_2). 4 mMol of CH_3NH_3I and 4 mMol of PbI_2 was dissolved in 10 mL of DMF/DMSO with V/V ratio 1/1. Then the substrate was heated up to 80 C and above solution dropped on the substrate and heated for 4-8 min.

Reversibility of perovskite film: We study degradation and its reversibility of perovskite film with direct contact with water drop. For this 2 μL of water was dropped on the surface of deposited perovskite film on different substrates. Then, it was heated up for 2 min at 80 C (please see the video in supporting information).

Degradation of perovskite film: Degradation of perovskite film was monitored by using XRD and DRS for three days in ambient atmosphere.

Computational method: We used Quantum Espresso package [49] based on the plane-wave basis set with a Cutoff Energy of 500 eV and the projector-augmented wave (PAW) pseudopotentials [50] and GGA for exchange-correlation functionals with PBE approach [51]. The partial occupancies for the total energy ground state calculation were calculated with smearing methodology with Methfessel-Paxton method and degauss value of 0.01 eV. The sampling of the Brillouin zone was done for the supercell with the equivalent of 2×2×1 Monkhorst-Pack [52] k-point mesh. Periodic boundary conditions were employed with a vacuum region of 10 Å between adjacent layers. In order to determine the equilibrium configuration of the interface, we relaxed all atomic coordinates and the supercell geometry using BFGS quasi-newton algorithm, based on the trust radius procedure and Davidson iterative diagonalization with overlap matrix Algorithm for SCF calculation. Also, we used the maximum residual force of less than 0.01 eV/Å. The sampling of the Brillouin zone was done for the supercell with the equivalent of 2×2×1 Monkhorst-Pack [49] k-point mesh.

Characterization: Scanning electron microscopy was carried out on a Hitachi SU8010 instrument operating at a 0.11.0 kV landing voltage. Powder X-ray diffraction was performed on a PANalytical Empyrean diffractometer configured with either a copper (Figure 6, λ = 1.54 Å) or cobalt (Figure S7, λ = 1.79 Å) X-ray source. UV-Vis absorbance spectra were acquired on a Cary 6000i spectrophotometer. Atomic force microscopy (AFM) model NT-MDT Solver P47 was used in tapping mode for morphological characterization using ultrasharp Si cantilevers.

Supporting Information

Supporting Information is available from the Wiley Online Library or from the author.

Acknowledgements

This work was supported in part by NSF (CMMI- 1727918).

Received: ((will be filled in by the editorial staff))
Revised: ((will be filled in by the editorial staff))
Published online: ((will be filled in by the editorial staff))

References

[1] A. Kojima, M. Teshima, Y. Shirai, T. Miyasaka, *J. Am. Chem. Soc.* **2009**, *131 (17)*, 6050–6051.

[2] J.-H. Im, J. Luo, M. Franckevičius, N. Pellet, P. Gao, T. Moehl, S. M. Zakeeruddin, M. K. Nazeeruddin, M. Grätzel, N.-G. Park, *Nano Lett*. **2015**, *15*, 2120-2126

[3] A. Mei, X. Li, L. Liu, Z. Ku, T. Liu, Y. Rong, M. Xu, M. Hu, J. Chen, Y. Yang, Science **2014**, *345*, 295-298.

[4] M. A. Green, A. Ho-Baillie, H. Snaith, *J. Nat. Photonics* **2014**, *8*, 506-514.

[5] K. Hwang, Y. S. Jung, Y. J. Heo, F. H. Scholes, S. E. Watkins, J. Subbiah, D. J. Jones,

D. Y. Kim, D. Vak, *Adv. Mater*. **2015**, *27*, 1241–1247.

[6] B. V. Lotsch, *Angew. Chem. Int. Ed*. **2014**, *53*, 635-637.

[7] W. Wang, D. Zhao, F. Zhang, L. Li, M. Du, Ch. Wang, Y. Yu, Q. Huang, M. Zhang, L. Li, J. Miao, Zh. Lou, G. Shen, *Adv. Funct. Mater*. **2017**, *27*, 1703953.

[8] J. Miao, F. Zhang, *J. Mater. Chem. C*. **2019**, *7*, 1741-1791.

[9] S. S. Shin, E. J. Yeom, W. S. Yang, S. Hur, M. G. Kim, J. Im, J. Seo, J. H. Noh, *Science* **2017**, *356*, 167–171.

[10] Q. Jiang, L. Zhang, H. Wang, X. Yang, J. Meng, H. Liu, Zh. Yin, J. Wu, X. Zhang, J. You, *Nat. Energy* **2017**, *2*, 16177.

[11] M. Saliba, T. Matsui, K. Domanski, J. Y. Seo, A. Ummadisingu, Sh. M. Zakeeruddin, *Science* **2016**, *354*, 206–209.

[12] D. Zhao, C. Chen, Ch. Wang, M. M. Junda, Zh. Song, C. R. Grice, Y. Yu, Ch. Li, B. Subedi, N. J. Podraza, X. Zhao, G. Fang, R. G. Xiong, K. Zhu, Y. Yan, *Nature Energy* **2018**, *3*, 1093-1100.

[13] https://www.nrel.gov/pv/cell-efficiency.html.

[14] J. Liu, Y. Wu, Ch. Qin, X. Yang, T. Yasuda, A. Islam, K. Zhang, W. Peng, W. Chena, L. Han, *Energy Environ. Sci*., **2014**, *7*, 2963.

[15] S. Habisreutinger, T. Leijtens, G. E. Eperon, S. Stranks, R. Nicholas, H. Snaith, *Nano Lett.* **2014**, *14*, 5561−5568.

[16] J. K. Kim, P. Liang, S. T. Williams, N. Cho, Ch. Chueh, M. S. Glaz , D. S. Ginger, A. Jen, *Adv. Mater*. **2014**, *27*, 695-701.

[17] T. Leijtens, G. Eperon, N. K. Noel, S. N. Habisreutinger, A. Petrozza, H. Snaith, *Adv. Energy Mater*. **2015**, *5*, 1500963.

[18] R. K. Misra, S. Aharon, B. Li, D. Mogilyansky, L. Visoly-Fisher, L. Etgar, E. A. Katz, J. *Phys. Chem. Lett.*, **2015**, *6 (3)*, 326–330.

[19] D. Bryant, N. Aristidou, S. Pont, L. Sanchez-Molina, Th. Chotchunangatchaval, S. Wheeler, J. R. Durrantab, S. A. Haque, *Energy Environ. Sci*., **2016**, *9*, 1655-1660

[20] X. Guo, C. McCleese, W. Gao, *Mater Renew Sustain Energy* **2016**, *5* 17-22.

[21] Z. Hawash, L. Ono, Q. Yabing, *Mater. Interfaces* **2018**, *5*, 1700623.

[22] M. Saliba, T. Matsui, J. Seo, K. Domanski, J. Correa-Baena, M. Kh. Nazeeruddin, Sh. M. Zakeeruddin, W. Tress, A. Abate, A. Hagfeldt, M. Grätz, *Energy Environ. Sci*., **2016**, *9*, 1989-1997.

[23] I. X. Smith, E. T. Hoke, D. Solis-Ibarra, M. D. McGehee, H. Karunadasa, *Angew. Chem. Int. Ed*. **2014**, *53*, 1 – 5.

[24] S. N. Habisreutinger, T. Leijtens, G. E. Eperon, S. Stranks, R. J. Nicholas, H. Snaith, *Nano Lett*. **2014**, *14*, 5561−5568.

[25] Ch. Chiang, M.K. Nazeeruddin, M. Grätzelc, Ch. Wu, *Energy Environ. Sci*., **2017**, *10*, 808-817.

[26] J. Yang, B. D. Siempelkamp, D. Liu, T. Kelly, *ACS Nano* **2015**, *9*, 1955–1963.

[28] X. Xu, K. Li, Zh. Yang, J. Shi, D. Li, L. Gu, Zh. Wu, Q. Meng, *Nano Research* **2016**, *10*, 250-257.

[29] B. Li, Y. Li, C. Zheng, D. Gao W. Huang, *RSC Adv*. **2016**, *6*, 38079-38091.

[30] Q.-D. Dao, R. Tsuji, A. Fujii, M. Ozaki, *Organic Electronics* **2017**, *43*, 229-234.

[31] S.-W. Lee, S. Kim, S. Bae, K. Cho, T. Chung, L. E. Mundt, S. Lee, S. Park, H. Park, M. C. Schubert, *Sci. Rep.* **2016**, *6*, 38150.

[32] Y. Kye, Ch. Yu, U. Jong, Y. Chen, A. Walsh, *J. Phys. Chem. Lett*. **2018**, *9 (9)*, 2196–2201.

[33] P. Sun, W. Chi, Z. Li, *Phys. Chem. Chem. Phys*. **2016**,*18*, 24526-24536.

[34] Zh. Song, A. Abate, S. Watthage, G. K. Liyanage, A. B. Phillips, U. Steiner, M. Graetzel, M. Heben, *Adv. Energy Mater*. **2016**, *12*, 1600846.

[35] W. Nie, J. Blancon, A. J. Neukirch, K. Appavoo, H. Tsai, *Nat. Commun*. **2016**, *7*, 11574.

[36] A. J. Pearson, G. Eperon, P. E. Hopkinson, S. N. Habisreutinger, J. Wang, H. Snaith, N. C. Greenham, *Adv. Energy Mater*. **2016**, *6*, 1600014.

[37] A. Farooq, I. M. Hossain, S. Moghadamzadeh, *ACS Appl. Mater. Interfaces*, **2018**, *10* (26), 21985–21990.

[38] G. Niu, W. Li, F. Meng, L. Wang, H. Dong, Y. Qiu, *J. Mater. Chem. A* **2014**, *2*, 705–710.

[39] S. Ito, S. Tanaka, K. Manabe, H. Nishino, *J. Phys. Chem. C* **2014**, *118*, 16995-17000.

[40] J. Yang, B. D. Siempelkamp, D. Liu, T. L. Kelly, *ACS Nano* **2015**, *9*, 1955-1963.

[41] B. Philippe, B. W. Park, R. Lindblad, J. Oscarsson, S. Ahmadi, E. M. Johansson, H. K. Rensmo, *Chem. Mater*. **2015**, *27*, 1720-1731

[42] L. Zhang, P. Sit, *J. Phys. Chem. C* **2015**, *119*, 22370–22378.

[43] W. Nie, J. Ch. Blancon, A. J. Neukirch, K. Appavoo, H. Tsai, M. Chhowalla, M.A. Alam,

Nat. Commun. **2016**, *7*, 11574.

[44] A. J. Pearson, G. E. Eperon, P. E. Hopkinson, S. N. Habisreutinger, J. T. Wang, H. J. Snaith, N. C. Greenham, *Adv. Energy Mater*. **2016**, *6*, 1600014.

[45] Y. Kye, Ch. Yu, U. Jong, Y. Chen, A. Walsh, *J. Phys. Chem. Lett*. **2018**, *9* (9), 2196–2201.

[46] C. Jing, B. Wu, R. Chen, Y. Wu, Y. Hui, B. Y. Mao, N. Zheng, *Adv. Mater.* **2018**, *30*, 1705596

[47] R. G. Pearson, *J. Am. Chem. Soc*. **1963**, *85*, 3533–3539.

[48] B. de. Courcy, L. G. Pedersen, O. Parisel, N. Gresh, B. Silvi, J. Pilmé, J. P. Piquemalm *J Chem Theory Comput.* **2010,** *6*, 1048–1063.

[49] P. Giannozzi, S. Baroni, N. Bonini, M. Calandra, R. Car, C. Cavazzoni, D. Ceresoli, G. L. Chiarotti, M. Cococcioni, I. Dabo, *J. Phys. Condens. Matter*. **2009**, *21* 395502.

[50] P.E. Blöchl, *Phys. Rev. B*. **1994**, *50*, 17953–17979.

[51] J. P. Perdew, K. Burke, M. Ernzerhof, *Phys. Rev. Lett.* **1996**, *77*, 3865–3868.

[52] H.J. Monkhorst, J.D. Pack, *Phys. Rev. B.* **1976**, *13*, 5188–5192.

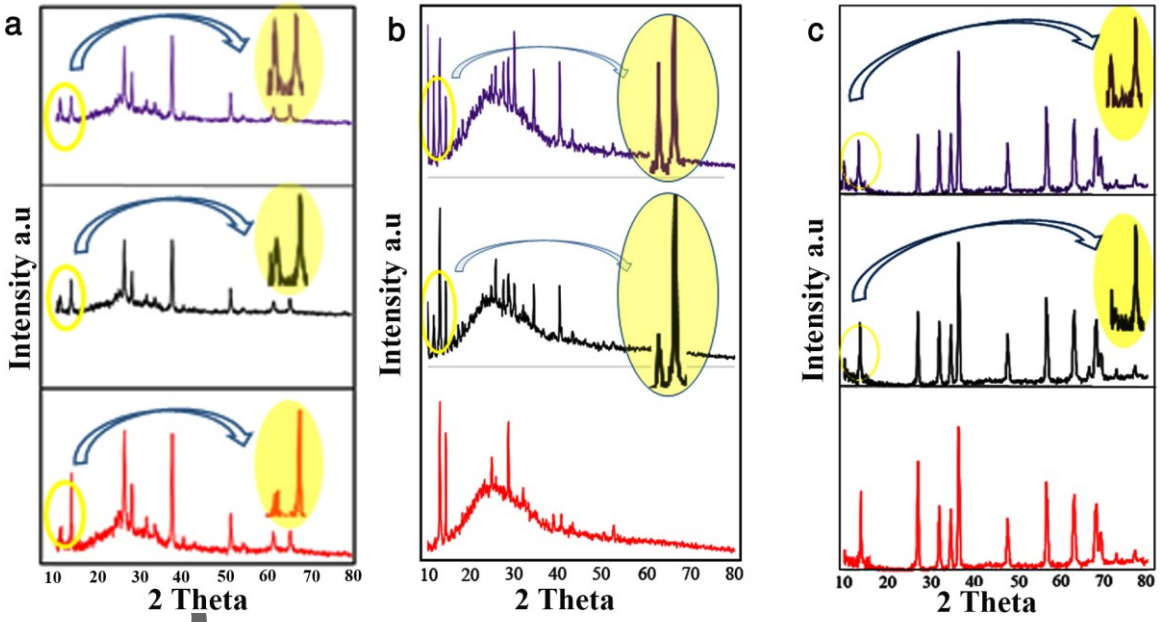

Figure 1. XRD pattern of perovskite absorber layer on a) TiO_2, b) compact ZnO and c) ZnO foil: first day (red), after 1 day (black), and after 2 days (purple)

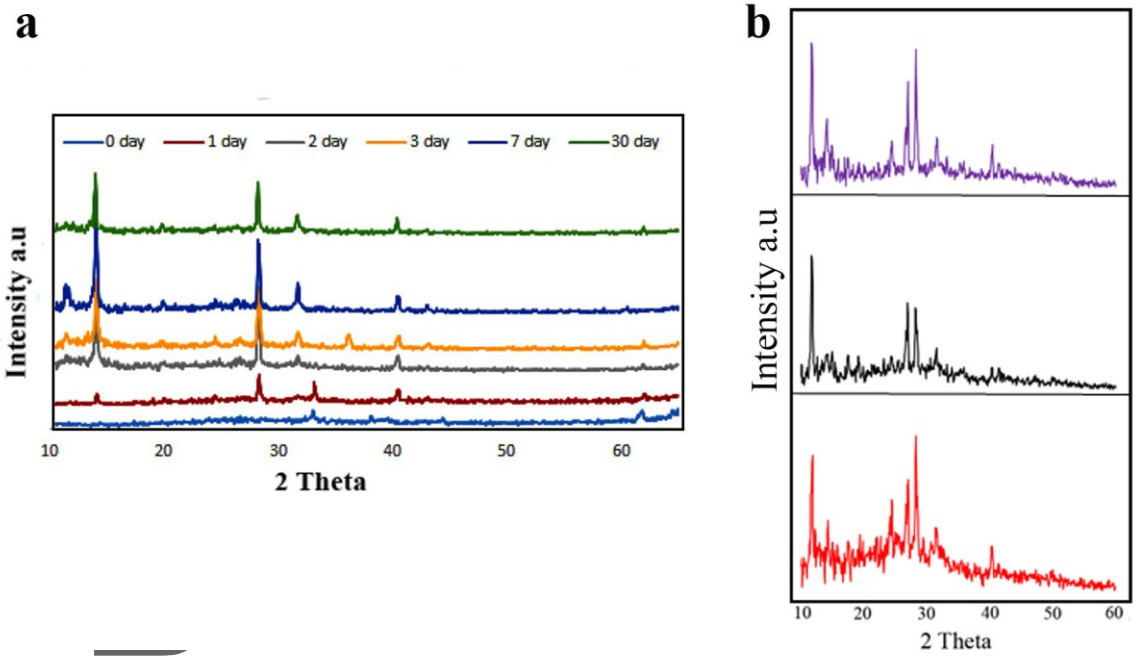

Figure 2. XRD pattern of perovskite absorber layer on: a) Si NWS and b) porous polysilicon.

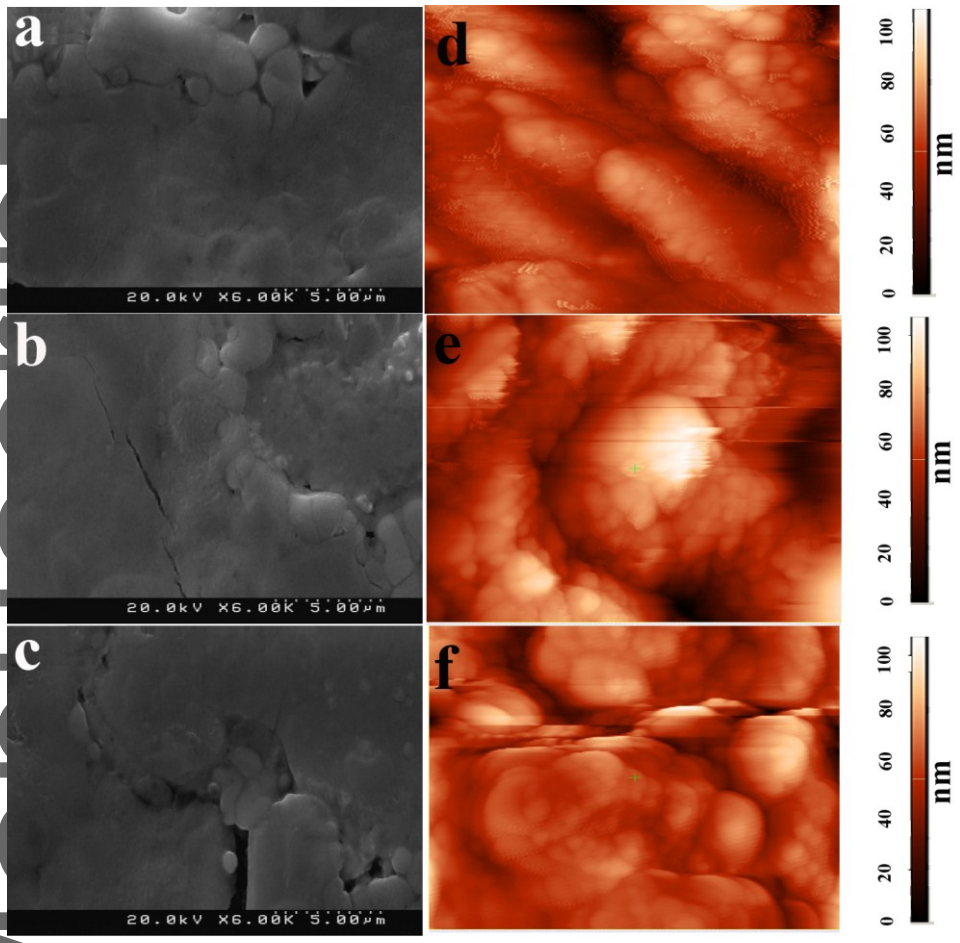

Figure 3. SEM (left) and AFM images (right) of $CH_3NH_3PbI_3$ on a) TiO_2, b) compact ZnO and c) porous polysilicon.

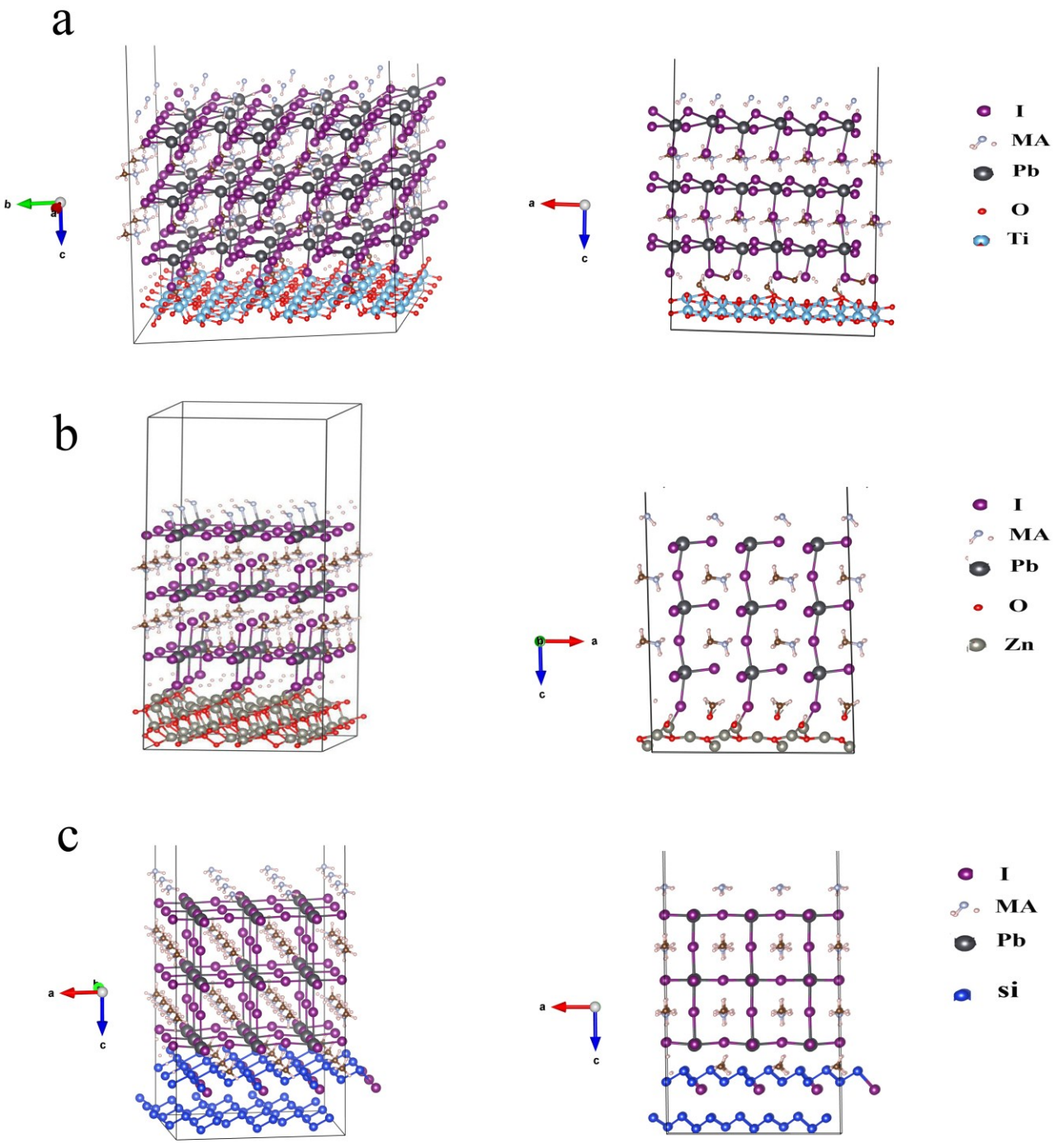

Figure 4. The optimized structures for a) $MAPbI_3/TiO_2$, b) $MAPbI_3/ZnO$ and c) $MAPbI_3/Si$.

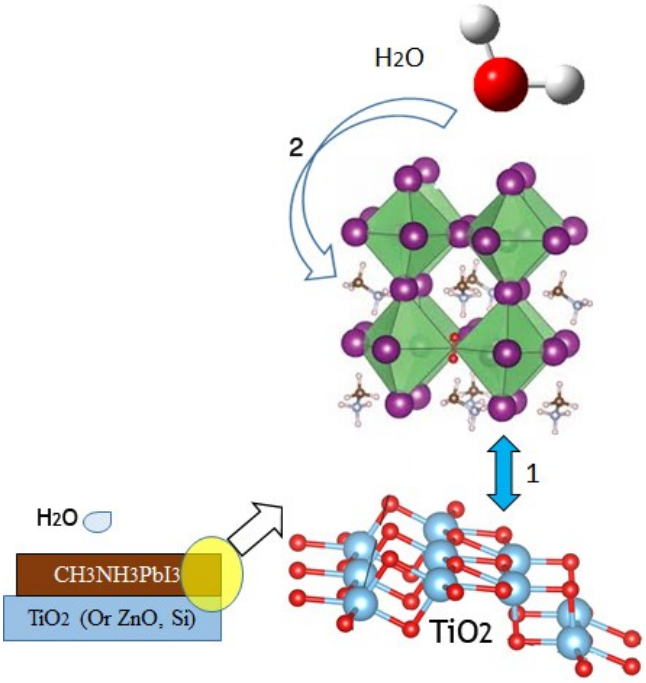

Figure 5 Degradation mechanism for $MAPbI_3$ on TiO_2 which started by interaction between perovskite layer and substrate.

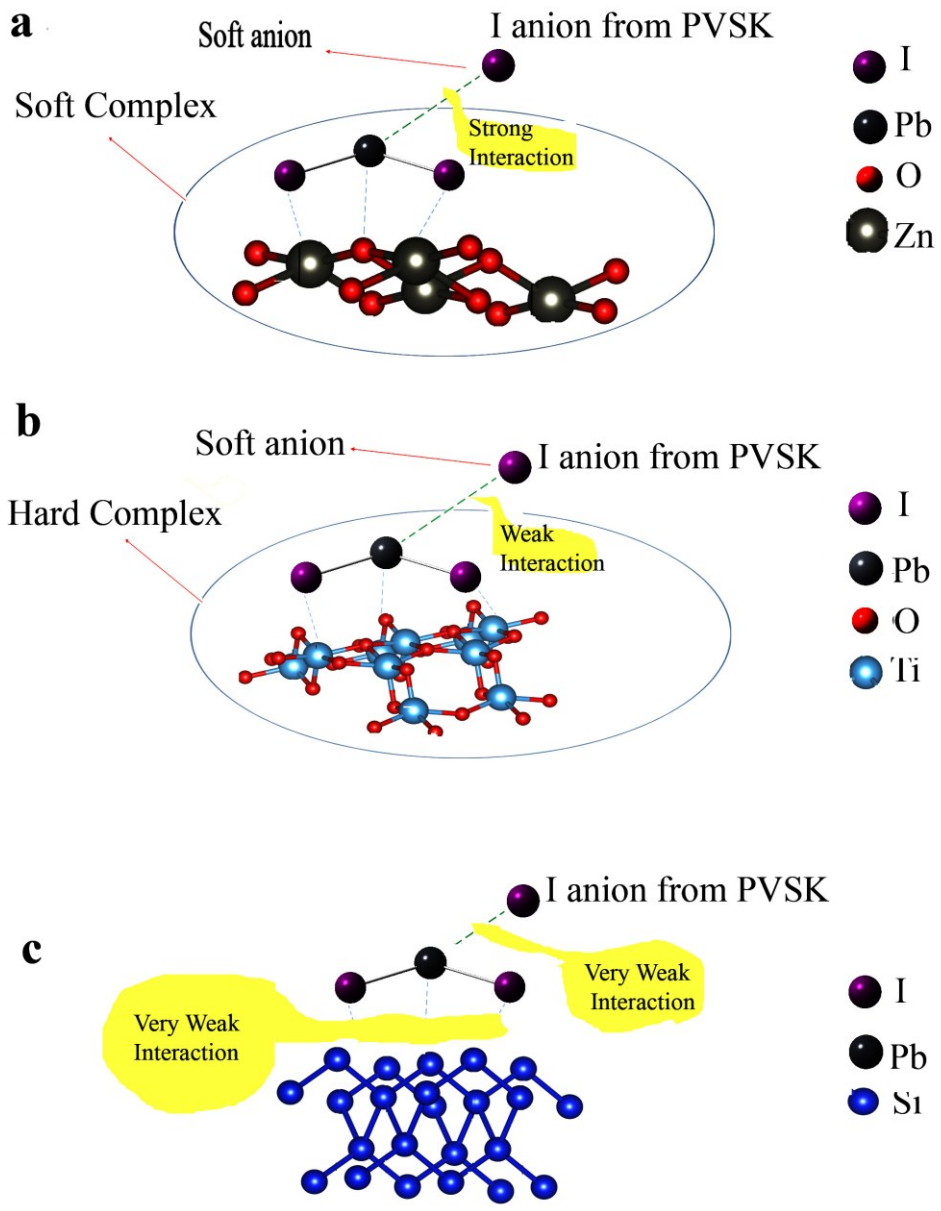

Figure 6. Schematic for formation of $MAPbI_3$ on a) TiO_2, b) ZnO and c) Si.

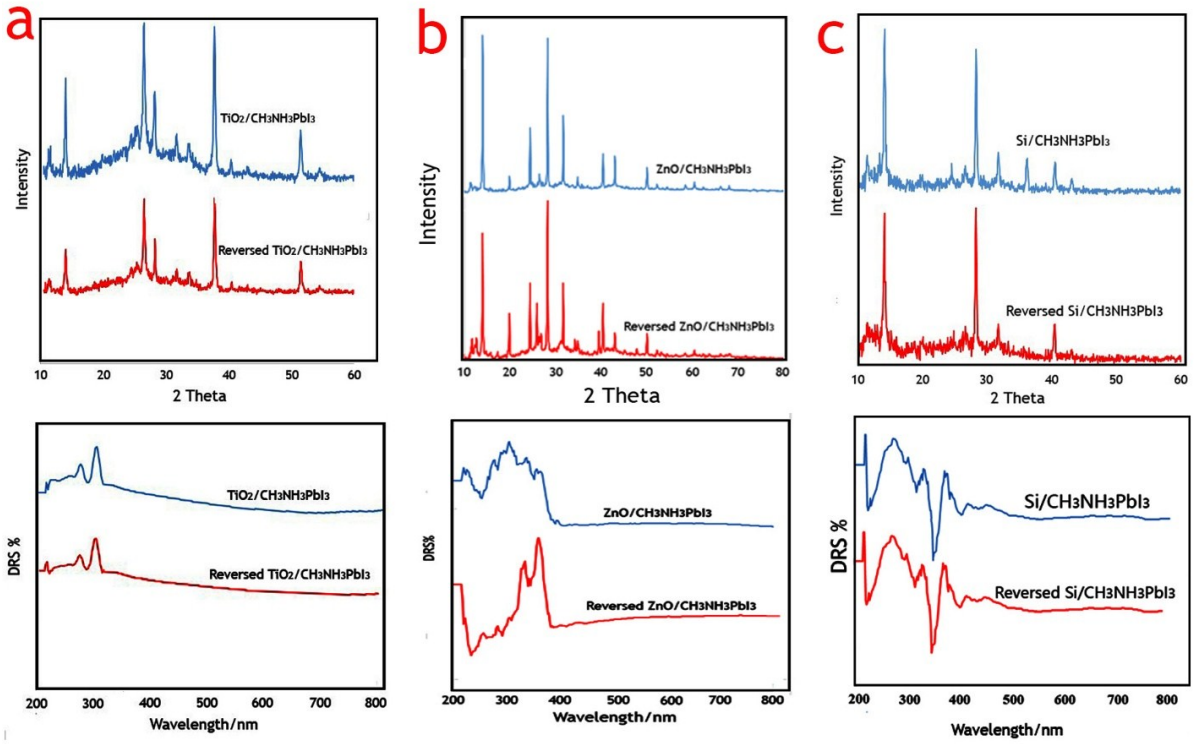

Figure 7. XRD and DRS $MAPbI_3$ and reversed $MAPbI_3$ on a) TiO_2, b) ZnO and c) Si. Red curve refers to the reversed $MAPbI_3$.

Commercial development of perovskite is seriously hindered by the instability of the perovskite. Therefore it is crucial to gain clear understanding of the mechanism of formation and degradation of perovskite in order to achieve stable perovskite devices. Base of theoretical and experimental results, we found that interaction between I atom in perovskite layer and substrate determine the stability of perovskite.